

Optimal Antenna Placement for Two-Antenna Near-Field Wireless Power Transfer

Kenneth MacSporran Mayer, Laura Cottatellucci, and Robert Schober
Friedrich-Alexander University Erlangen-Nuremberg, Germany

Abstract—Current trends in communication system design precipitate a change in the operating regime from the traditional far-field to the radiating near-field (Fresnel) region. We investigate the optimal transmit antenna placement for a multiple-input single-output (MISO) wireless power transfer (WPT) system designed for a three-dimensional cuboid room under line-of-sight (LoS) conditions in the Fresnel region. We formulate an optimisation problem for maximising the received power at the worst possible receiver location by considering the spherical nature of the electromagnetic (EM) wavefronts in the Fresnel region while assuming perfect knowledge of the channel at the transmitter. For the case of two transmit antennas, we derive a closed-form expression for the optimal positioning of the antennas which is purely determined by the geometry of the environment. If the room contains locations where the far-field approximation holds, the proposed positioning is shown to reduce to the far-field solution. The analytical solution is validated through simulation. Furthermore, the maximum received power at the locations yielding the worst performance is quantified and the power gain over the optimal far-field solution is presented. For the considered cuboid environment, we show that a distributed antenna system is optimal in the Fresnel region, whereas a co-located antenna architecture is ideal for the far-field.

I. INTRODUCTION

Future communication systems are moving towards operating at higher frequencies, as the associated large bandwidth helps support the ever-increasing requirements on data rate, low latency, network heterogeneity, as well as energy efficiency. This precipitates a change in the operating regime from the traditional far-field to the radiating near-field (Fresnel) region, which must be reflected in the modelling of the wireless channel [1]. Wireless systems designed for the Fresnel region are of interest not only for communications [2], but also for wireless power transfer (WPT) [3]. WPT systems designed for the Fresnel region are capable of focusing the energy beams for transferring power wirelessly, thus yielding a larger amount of received power and causing less energy pollution in unwanted directions compared to traditional far-field approaches [1], [3].

A key difference between the far-field and the radiating near-field is how the electromagnetic (EM) wavefronts are modelled. While a planar wavefront model (PWM) is suitable for the far-field, considering the spherical nature of the EM wavefronts is indispensable in the Fresnel region [1]. Therefore, the design of wireless systems for the radiating near-field is driven by the spherical wavefront model (SWM) [1]–

[3]. The SWM has been considered for WPT in [4] where a dynamic metasurface antenna is employed to maximise the weighted sum of received energies via beam focusing.

While the study of WPT in the Fresnel region is at an early stage, far-field WPT has been extensively studied. A comprehensive overview of the design concepts, capabilities and limitations, prototypes, and applications of WPT systems is provided in [5]–[11]. Typically, WPT systems are required to have line-of-sight (LoS) between transmitter and receiver in order to attain adequate power transfer efficiency [10]. Additionally, in state-of-the-art WPT systems, the transmit antennas of the energy transmitter are either co-located or distributed [10]. Co-located antenna architectures have been employed, for example, in [12] and distributed antenna systems (DASs) have been considered in [13], [14]. DASs are an appealing transmit antenna architecture for WPT systems and enable cooperation among the distributed transmit antennas. Compared to co-located energy transmitters, employing a DAS results in a more uniform distribution of the received power in the environment [10]. DASs for WPT have been investigated for different transmission strategies such as transmit antenna selection [14] and maximum ratio transmission [13].

In this paper, we consider a multiple-input single-output (MISO) WPT system that comprises a two-antenna energy transmitter and a single antenna energy receiver in LoS conditions. The energy receiver is located at an arbitrary position in a three-dimensional cuboid room and the transmit antennas are located on one of the room's walls. We determine the amplitude variations of the wireless channel based on geometrical considerations and optimise the positions of the transmit antennas analytically, thereby showing whether a co-located or a distributed transmit antenna architecture is optimal. Hereby, the objective is to maximise the received power for the worst possible receiver position. Thus, the proposed solution ensures provision of the maximum, worst-case power for the given environment when there is no prior knowledge on the receiver's location in the room. This is crucial for wirelessly powered devices utilised for continuous monitoring, such as sensors and wearables.

Our approach for optimising the transmit antenna positions of a WPT system is designed for a three-dimensional cuboid room and relies on exploiting the spherical nature of the EM wavefronts. Therefore, the existing results [5]–[14] which were obtained for WPT systems designed for the far-field operating regime are not applicable to the problem considered in this paper. The antenna placement problem is formulated

The work was supported in part by the German Research Foundation through Project SFB 1483.

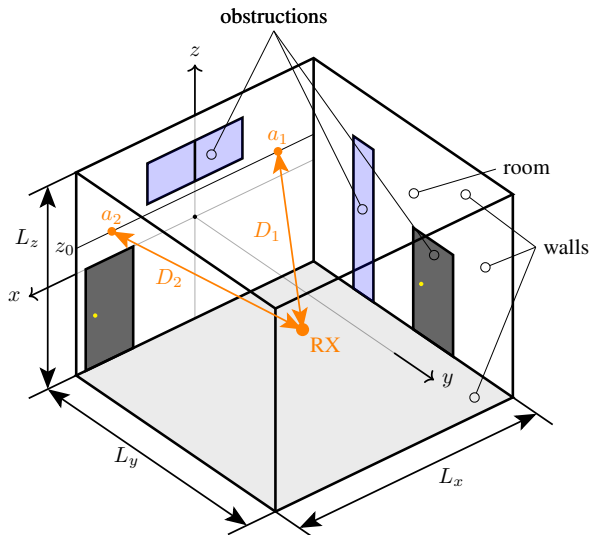


Fig. 1: Illustration of the system model with two transmit antennas, i.e., $N_t = 2$. The receiver (RX) is located in a cuboid room, where portions of the wall are obstructed. The transmit antennas are located on a horizontal line at a_1 and a_2 . The distance to the receiver is given by D_1 and D_2 , respectively.

for a general number of transmit antennas and we solve the problem optimally for a two-antenna system. The analytical expression describing the optimal transmit antenna positions only depends on the geometry of the environment. While the proposed solution is designed around capturing the effects of the spherical EM wavefronts in the Fresnel region, the solution is shown to converge to the optimal far-field solution once the distances are large enough for the PWM to become sufficiently accurate at the worst possible receiver positions. The proposed optimal transmit antenna deployment reveals that a DAS is the optimal transmit antenna architecture in the Fresnel region, whereas a co-located architecture is optimal in the far-field. The point of transition between the DAS and the co-located transmit antenna architecture is determined through geometrical considerations. Moreover, the extension of the presented methodology to systems with more than two transmit antennas is briefly discussed. The analytical solution is validated by solving the problem numerically. Furthermore, the power gain over the far-field solution is investigated which shows that, in the Fresnel region, deploying a DAS results in up to three times as much received energy at the receiver compared to a co-located architecture.

II. SYSTEM MODEL

The WPT system considered in this paper comprises a transmitter equipped with N_t antennas and a single-antenna receiver endowed with an energy harvester. An illustration of the environment is provided in Fig. 1 for $N_t = 2$.

A. Environment

The considered environment is a three-dimensional cuboid room which is defined by the Cartesian product of the sets \mathcal{X} ,

\mathcal{Y} , and \mathcal{Z} , i.e., $\mathcal{X} \times \mathcal{Y} \times \mathcal{Z}$, with

$$\mathcal{X} = \left\{ x \mid -\frac{L_x}{2} \leq x \leq \frac{L_x}{2} \text{ with } L_x > 0 \right\}, \quad (1)$$

$$\mathcal{Y} = \{ y \mid 0 \leq y \leq L_y \text{ with } L_y > 0 \}, \quad (2)$$

and

$$\mathcal{Z} = \left\{ z \mid -\frac{L_z}{2} \leq z \leq \frac{L_z}{2} \text{ with } L_z > 0 \right\}. \quad (3)$$

The receiver, e.g., a wearable device, relies on being powered wirelessly and is assumed to be located at an arbitrary position in the environment. The receiver location is defined by the triplet $(x, y, z) \in \mathcal{X} \times \mathcal{Y} \times \mathcal{Z}$.

B. Transmit Antenna Model

Identical and omnidirectional transmit antennas are employed to illuminate the entire room since the receiver may be located anywhere in the environment. The location of transmit antenna i is described by the triplet $(a_{ix}, a_{iy}, a_{iz}) \in \mathcal{X} \times \mathcal{Y} \times \mathcal{Z}$, $\forall i = 1, \dots, N_t$. The amount of power obtained at the receiver is shown to depend on the placement of the transmit antennas in Subsection II-C. Consequently, the amount of power at the receiver can be maximised by optimising the positions of the transmit antennas.

There is an inherent trade-off between the achievable performance and the practicality of the transmit antenna deployment. Although leveraging the full potential of a flexible placement would yield the best performance, the resulting transmit antenna locations may be impractical or even infeasible in practice. Therefore, we restrict the antennas to being placed along a horizontal line defined by $y = 0, z = z_0 \in \mathcal{Z}$. Consequently, the transmit antenna positions are restricted in the environment through the following condition

$$\forall i = 1, \dots, N_t : a_{ix} \in \mathcal{X}, a_{iy} = 0, a_{iz} = z_0 \in \mathcal{Z}. \quad (4)$$

Throughout this paper, a_{ix} is denoted by a_i for simplicity of notation.

C. Channel and Signal Model

The Fresnel region of a wireless system is defined, e.g., in [2], and depends on the relationship between the wavelength of the EM waves and the distance between the transmit antennas in comparison to their distance from the receiver. The size of the Fresnel region increases with the carrier frequency. While the Fresnel region is negligibly small in conventional wireless systems, when using mmWave frequency bands or higher, the size of the Fresnel region becomes relevant, e.g., for indoor scenarios. Furthermore, for high carrier frequencies, the severe reflection and scattering losses cause the wireless channel to become predominantly LoS [1], [3], [15]. A LoS channel is typically assumed for wireless systems operating in the Fresnel region [2], [3], [16].

LoS between transmitter and receiver allows a WPT system to attain adequate power transfer efficiency [10]. On the other

hand, we note that LoS channels are susceptible to blockages [3]. For analytical tractability of system design, we make the assumption that a LoS connection between the transmit antennas and the receiver exists and do not consider the impact of channel blockages in this paper.

Based on the previous considerations, free-space LoS propagation of the EM wavefronts is considered in this paper.

When considering free-space LoS conditions, the equivalent complex baseband channel between transmit antenna i and the receiver is given by [17]

$$g_i = \frac{\sqrt{c}}{D_i} e^{-j\frac{2\pi}{\lambda} D_i}, \quad (5)$$

where λ is the wavelength, D_i is the distance between transmit antenna i and the receiver, and c is the channel power gain at the reference distance of 1 meter. Since the wireless channel of the considered MISO system is modelled using the SWM, both the amplitude and the phase of g_i depend on distance D_i . In contrast, for the PWM, the *path loss* between all transmit antennas and the receiver is assumed to be constant, i.e., $D_i \approx D, \forall i = 1 \dots N_t$. The MISO channel is represented by the N_t -dimensional vector $\mathbf{g} = [g_1, \dots, g_{N_t}]^T \in \mathbb{C}^{N_t \times 1}$. The channel model in (5) has been considered for describing systems designed for the Fresnel region in [16] and was adapted for the case of directional antennas in [2], [3].

In [18], it was shown that the received power γ for any given position in the environment is maximised by transmitting vector $\mathbf{s} = \sqrt{P} \mathbf{g} / \|\mathbf{g}\|_2 \in \mathbb{C}^{N_t \times 1}$ over the N_t transmit antennas, where P is the total transmit power, which is shared among the antennas, and $\|\cdot\|_2$ is the Euclidean norm. Therefore, the received power γ is given by

$$\gamma = \|\mathbf{g}^H \mathbf{s}\|_2^2 = P \|\mathbf{g}\|_2^2 = Pc \sum_{i=1}^{N_t} \frac{1}{D_i^2}. \quad (6)$$

Thus, the received power is directly proportional to the sum of the squared, inverse distances between the receiver and the transmit antennas. While the method in [18] was designed for steering beams in the far-field, it also applies to focusing energy beams towards the receiver in the Fresnel region [2]. Note that the impact of additive noise on the received power is negligible.

III. PROBLEM FORMULATION AND OPTIMAL SOLUTION

A. Problem Formulation

The objective is to deploy the transmit antennas such that the receiver is powered reliably anywhere in the environment. Analytically, this is attained by determining the optimal transmit antenna placement, which satisfies the constraints imposed on the positions in Section II-B, such that the received power γ is maximised at the worst possible receiver location. Supposing the i -th transmit antenna and the receiver are located at positions $(a_i, 0, z_0)$ and (x, y, z) , respectively, then

the received power γ , defined in (6), is proportional to the following function

$$f_{xyz}(a_1, \dots, a_{N_t}) = \sum_{i=1}^{N_t} \frac{1}{(x - a_i)^2 + y^2 + (z - z_0)^2}, \quad (7)$$

which depends on the transmit antenna positions. The proposed design is obtained as the solution of the following maxim problem

$$\underset{a_1, \dots, a_{N_t}}{\text{maximise}} \quad \min_{x, y, z} f_{xyz}(a_1, \dots, a_{N_t}) \quad (8a)$$

$$\text{subject to} \quad (1), (2), (3), (4), \quad (8b)$$

which is non-convex due to the objective function in (8a). Note that (7) is independent of the wavelength, which is required to define the Fresnel region of a wireless system [2]. Here, we assume the wavelength of the system is chosen such that the system is operating in the Fresnel region for a given transmit antenna placement.

By first identifying the receiver locations resulting in the worst performance independent of the transmit antenna positions, the complexity of the problem can be reduced. The set containing these critical receiver locations is denoted by $\mathcal{X}^{\text{crit}} \times \mathcal{Y}^{\text{crit}} \times \mathcal{Z}^{\text{crit}}$, where $\mathcal{X}^{\text{crit}} \subset \mathcal{X}$, $\mathcal{Y}^{\text{crit}} \subset \mathcal{Y}$, and $\mathcal{Z}^{\text{crit}} \subset \mathcal{Z}$.

Proposition 1. *It suffices to consider the receiver locations defined by $y = L_y$, $z = -L_z/2$ and $y = L_y$, $z = L_z/2$ for optimisation problem (8). $\mathcal{Z}^{\text{crit}}$ is given by $\mathcal{Z}^{\text{crit}} = \{-L_z/2\}$ if $0 \leq z_0 \leq L_z/2$ and $\mathcal{Z}^{\text{crit}} = \{L_z/2\}$ if $-L_z/2 \leq z_0 \leq 0$. $\mathcal{Y}^{\text{crit}}$ is given by $\mathcal{Y}^{\text{crit}} = \{L_y\}$.*

Proof. Since (7) is a monotonically decreasing function of y and $|z - z_0|$, the worst objective value is obtained at the lines at $y = L_y$, $z = -L_z/2$ if $0 \leq z_0 \leq L_z/2$ and $y = L_y$, $z = L_z/2$ if $-L_z/2 \leq z_0 \leq 0$. Therefore, the critical sets are given by $\mathcal{Y}^{\text{crit}} = \{L_y\}$ and $\mathcal{Z}^{\text{crit}} = \{-L_z/2\}$ if $z_0 \geq 0$ and $\mathcal{Z}^{\text{crit}} = \{L_z/2\}$ if $z_0 \leq 0$. \square

$\mathcal{X}^{\text{crit}}$ cannot be obtained based on monotonicity due to the dependency between the receiver location and the transmit antenna variables in (7). Restricting the receiver positions to the critical set and defining $L'_z = L_z + 2|z_0|$, allows the following equivalent reformulation of (7)

$$f_x(a_1, \dots, a_{N_t}) = \sum_{i=1}^{N_t} \frac{1}{(x - a_i)^2 + L_y^2 + \frac{L'_z{}^2}{4}}, \quad (9)$$

which is independent of variables y and z . Finally, (8) is equivalently reformulated as

$$\underset{a_1, \dots, a_{N_t}}{\text{maximise}} \quad \min_x f_x(a_1, \dots, a_{N_t}) \quad (10a)$$

$$\text{subject to} \quad (1), (4). \quad (10b)$$

B. Optimal Solution

For the remainder of this paper, the number of transmit antennas is set to $N_t = 2$. This allows for an intuitive illustration of the geometrical considerations underlying the

proposed method, thus offering insight into the solution structure of the considered transmit antenna placement problem. The application of the method presented in this paper to systems with $N_t > 2$ is discussed in Subsection III-D. In the following, the symmetry of f_x in (9) is investigated in Proposition 2.

Proposition 2. *For $N_t = 2$, the optimal locations of the transmit antennas a_1 and a_2 must satisfy $a_1^* = -a_2^*$.*

Proof. For any $a_1, a_2 \in \mathcal{X}$ with $a_2 > a_1$, the α -superlevel set of f_x is defined as

$$S_\alpha(f_x) = \{x \in \mathcal{X} \mid f_x(a_1, a_1 + m) \geq \alpha\}, \quad (11)$$

where $m = a_2 - a_1$. By inspection, the set $S_\alpha(f_x)$ is symmetrical around the plane $x = a_1 + m/2$ for any choice of α . The max-min problem (10) is equivalent to maximising the infimum of $S_\alpha(f_x)$ with respect to (w.r.t.) α while forcing $S_\alpha(f_x)$ to envelope the whole environment $\mathcal{X} \times \mathcal{Y} \times \mathcal{Z}$. This is equivalent to the following optimisation problem

$$\underset{\alpha}{\text{maximise}} \quad \inf S_\alpha(f_x) \quad (12a)$$

$$\text{subject to} \quad \mathcal{X} \times \mathcal{Y} \times \mathcal{Z} \subseteq S_\alpha(f_x). \quad (12b)$$

Since the amount of received power decreases as the distance between the receiver and the transmit antennas increases, the level sets departing from the transmit antenna positions must decrease. Since $S_\alpha(f_x)$ must encapsulate the entire room, the maximum value of α is only attained if the symmetry plane passes through the point $(0, 0, a_{z_0})$, i.e., $a_1 + m/2 = 0$, which implies $a_1^* = -a_2^*$. Intuitively any other choice of x , i.e. $0 \neq x = a_1 + m/2$, would bias some receiver positions over others, thus causing the performance at the worst position to decrease. \square

Proposition 2 allows dropping the dependency on a_2 in the objective function f_x , i.e., $f_x(a_1, a_2) = f_x(a_1)$, with $a_2 = -a_1$. For a given x , the optimal transmit antenna positions are obtained by determining the stationary points of function $f_x(a_1)$ as follows

$$\frac{\partial f_x(a_1)}{\partial a_1} \stackrel{!}{=} 0. \quad (13)$$

Solving (13) for a_1 , five stationary points $a_1^\beta(x, L_y, L'_z)$, $\beta \in \{\text{(I)}, \text{(II)}, \text{(III)}, \text{(IV)}, \text{(V)}\}$, are found and given in the following

$$\begin{aligned} a_1^{(\text{I})}(x, L_y, L'_z) &= \frac{1}{2} \sqrt{e(x, L_y, L'_z) - d(x, L_y, L'_z)} \\ &= -a_1^{(\text{II})}(x, L_y, L'_z), \end{aligned} \quad (14)$$

$$\begin{aligned} a_1^{(\text{III})}(x, L_y, L'_z) &= \frac{1}{2} \sqrt{-e(x, L_y, L'_z) - d(x, L_y, L'_z)} \\ &= -a_1^{(\text{IV})}(x, L_y, L'_z), \end{aligned} \quad (15)$$

$$a_1^{(\text{V})}(x, L_y, L'_z) = 0, \quad (16)$$

where $e(x, L_y, L'_z) = 4x\sqrt{4x^2 + 4L_y^2 + L'_z{}^2}$ and $d(x, L_y, L'_z) = (4x^2 + 4L_y^2 + L'_z{}^2)$. Using the symmetrical relationships $e(-x, L_y, L'_z) = -e(x, L_y, L'_z)$ and $d(-x, L_y, L'_z) = d(x, L_y, L'_z)$, we obtain $a_1^{(\text{III})}(x, L_y, L'_z) = a_1^{(\text{I})}(-x, L_y, L'_z)$ and $a_1^{(\text{IV})}(x, L_y, L'_z) = a_1^{(\text{II})}(-x, L_y, L'_z)$. Thus, it is sufficient to investigate the three stationary points $a_1^{(\text{I})}(x, L_y, L'_z)$, $a_1^{(\text{II})}(x, L_y, L'_z)$, and $a_1^{(\text{V})}(x, L_y, L'_z)$. Additionally, due to the symmetrical relationship between the antennas, i.e., $a_2 = -a_1$, $a_1^{(\text{II})}(x, L_y, L'_z)$ is also redundant.

Proposition 3. *If the geometry of the environment satisfies $4(L_y/L_x)^2 + (L'_z/L_x)^2 \geq 3$, the optimal transmit antenna positions are $a_1^* = a_2^* = 0$, otherwise they satisfy $a_1^* = -a_2^* \neq 0$.*

Proof. The optimal antenna positions must be real numbers. While the stationary point $a_1^{(\text{V})}$ is always real, $a_1^{(\text{I})}(x, L_y, L'_z)$ is only real and different from $a_1^{(\text{V})}(x, L_y, L'_z)$, if $e(x, L_y, L'_z) > d(x, L_y, L'_z)$ is satisfied. This holds for

$$|x| > \sqrt{\frac{L'_z{}^2}{12} + \frac{L_y^2}{3}}. \quad (17)$$

Consequently, if the inequality in (17) does not hold, then (14) is complex, and thus, unsuitable for describing antenna locations. If the inequality does not hold for the largest possible value of x , it does not hold for any value of x . Therefore, by inserting $x = L_x/2$ into (17), a condition purely in terms of the geometry of the system is established:

$$4\frac{L_y^2}{L_x^2} + \frac{L'_z{}^2}{L_x^2} \geq 3. \quad (18)$$

If (18) is satisfied, then only $a_1^{(\text{V})}(x, L_y)$ is real and the optimal positions for both antennas are $a_1 = a_2 = 0$. However, if $4(L_y/L_x)^2 + (L'_z/L_x)^2 < 3$ holds, then $a_1^{(\text{I})}(x, L_y, L'_z)$ is real and different from zero. \square

In summary, Proposition 3 shows that a co-located or a distributed antenna architecture is optimal depending on a linear combination of the ratios L_y/L_x and L'_z/L_x .

Lemma 1. *If the geometry of the environment satisfies $4(L_y/L_x)^2 + (L'_z/L_x)^2 \geq 3$, then $\mathcal{X}^{\text{crit}} = \{-L_x/2, L_x/2\}$.*

Proof. Every term in the function f_x is the inverse of a quadratic function [19]. Since f_x is a (positive) sum of two positive terms, f_x must also be positive for all inputs, i.e., $\forall x, \forall a_1 : f_x(a_1) > 0$.

Suppose $a_1^{(\text{V})}$ is the only real stationary point, i.e., (18) is satisfied. The global maximum is reached at $a_1^{(\text{V})}$, since only positive values contribute to f_x . Since there are no other stationary points, the function decays monotonically from the maximum. Therefore, the lowest values occur at the boundaries of \mathcal{X} , i.e., $x = -L_x/2 = L_x/2$. Thus, $\mathcal{X}^{\text{crit}} = \{-L_x/2, L_x/2\}$. \square

Lemma 2. *If $4(L_y/L_x)^2 + (L'_z/L_x)^2 < 3$, the critical points $\mathcal{X}^{\text{crit}}$ are either $\mathcal{X}^{\text{crit}} = \{-L_x/2, L_x/2\}$ or $\mathcal{X}^{\text{crit}} =$*

$\{-L_x/2, 0, L_x/2\}$. The optimal transmit antenna positions are given by

$$a_1^* = \frac{L_x}{2} \sqrt{2 \sqrt{4 \frac{L_y^2}{L_x^2} + \frac{L_z'^2}{L_x^2} + 1} - \left(4 \frac{L_y^2}{L_x^2} + \frac{L_z'^2}{L_x^2} + 1\right)}, \quad (19)$$

and

$$a_1^* = \frac{L_x}{2} \frac{\sqrt{4 \frac{L_y^2}{L_x^2} + \frac{L_z'^2}{L_x^2} + 1}}{\sqrt{3}}, \quad (20)$$

in the former and the latter case, respectively.

Proof. If (18) is not satisfied, then f_x has real stationary points at $a_1^{(I)} = -a_1^{(III)}$ and $a_1^{(V)}$. As the superposition of inverse quadratic functions, f_x is asymptotic to zero when the function's argument goes to infinity [19]. Consequently, $a_1^{(I)} = -a_1^{(III)}$ must be maxima. Since the value of the function decays monotonically from any maximum, and $a_1^{(V)}$ is a stationary point which lies exactly between the two maxima, it must be a local minimum. This is due to the symmetry of f_x around the centre of \mathcal{X} . In this case, two scenarios are possible. Either $x = -L_x/2 = L_x/2$ remains to be the worst possible location (as in Lemma 1) or the objective value at an additional, different x location becomes critical. In the first case, the critical set becomes $\mathcal{X}^{\text{crit}} = \{-L_x/2, L_x/2\}$. The optimal transmit antenna position for a_1^* is obtained by inserting $x = L_x/2$ into (14) which yields (19). The latter case occurs when the transmit antennas are moved so far towards the boundaries of \mathcal{X} that the performance is favoured there, causing the performance at the origin to decrease the most. Consequently, the worst performance is achieved either at the extremes or at the centre of the interval \mathcal{X} . In this case, the set of critical values $\mathcal{X}^{\text{crit}}$ becomes $\mathcal{X}^{\text{crit}} = \{-L_x/2, 0, L_x/2\}$. By definition, the performance at the critical points $x \in \mathcal{X}^{\text{crit}}$ is worst. Therefore, the performance at all critical points must be identical. Since $f_{-L_x/2}(a_1) = f_{L_x/2}(a_1)$ holds for any a_1 by symmetry, it is sufficient to investigate the equality

$$f_0(a_1^*) \stackrel{!}{=} f_{\frac{L_x}{2}}(a_1^*) \quad (21)$$

which implies (20). \square

From Lemma 2 it follows that a_1^* depends purely on the geometry of the system. Next, in Lemma 3 a condition on the geometry is established which describes the point of transition from (19) to (20).

Lemma 3. *The point of transition between (19) and (20) occurs at $4(L_y/L_x)^2 + (L_z'/L_x)^2 = 5/4$.*

Proof. The point of transition is identified by equating (19) and (20). \square

Proposition 4. *The optimal transmit antenna position a_1^* such that the received power γ is maximised at the worst receiver position in the environment is given by*

$$a_1^* = \begin{cases} (20) & \text{if } 4 \frac{L_y^2}{L_x^2} + \frac{L_z'^2}{L_x^2} \leq \frac{5}{4}, \\ (19) & \text{if } \frac{5}{4} \leq 4 \frac{L_y^2}{L_x^2} + \frac{L_z'^2}{L_x^2} \leq 3, \\ 0 & \text{if } 4 \frac{L_y^2}{L_x^2} + \frac{L_z'^2}{L_x^2} \geq 3. \end{cases} \quad (22)$$

Proof. The proof follows from Lemma 2, Lemma 3, and (14). \square

Corollary 1. *The optimal transmit antenna deployment, defined in Proposition 4, yields the maximum received power γ^* for the worst receiver position which is given by*

$$\gamma^* = Pc \begin{cases} \frac{2}{\frac{4}{3}L_y^2 + \frac{1}{12}L_x^2 + \frac{1}{3}L_z'^2} & \text{if } 4 \frac{L_y^2}{L_x^2} + \frac{L_z'^2}{L_x^2} \leq \frac{5}{4}, \\ \frac{2 \sqrt{4 \frac{L_y^2}{L_x^2} + \frac{L_z'^2}{L_x^2} + 1} + 2}{4L_y^2 + L_z'^2} & \text{if } \frac{5}{4} \leq 4 \frac{L_y^2}{L_x^2} + \frac{L_z'^2}{L_x^2} \leq 3, \\ \frac{2}{L_y^2 + \frac{1}{4}L_x^2 + \frac{1}{4}L_z'^2} & \text{if } 4 \frac{L_y^2}{L_x^2} + \frac{L_z'^2}{L_x^2} \geq 3. \end{cases} \quad (23)$$

Proof. The received power γ^* is obtained by inserting (7) into (6) for the optimal transmit antenna positions (22)

$$\gamma^* = Pc f_x(a_1^*, a_2^*), \quad (24)$$

where $f_x(a_1^*, a_2^*)$ is the optimal objective value of the optimisation problem in (10). The objective value is obtained by inserting (22) into (9) and evaluating the resulting function at $x \in \mathcal{X}^{\text{crit}}$. Then, $f_x(a_1^*, a_2^*)$ is given by

$$\frac{2}{\frac{4}{3}L_y^2 + \frac{1}{12}L_x^2 + \frac{1}{3}L_z'^2} \quad \text{if } 4 \frac{L_y^2}{L_x^2} + \frac{L_z'^2}{L_x^2} \leq \frac{5}{4}, \quad (25)$$

$$\frac{2 \sqrt{4 \frac{L_y^2}{L_x^2} + \frac{L_z'^2}{L_x^2} + 1} + 2}{4L_y^2 + L_z'^2} \quad \text{if } \frac{5}{4} \leq 4 \frac{L_y^2}{L_x^2} + \frac{L_z'^2}{L_x^2} \leq 3, \quad (26)$$

and

$$\frac{2}{L_y^2 + \frac{1}{4}L_x^2 + \frac{1}{4}L_z'^2} \quad \text{if } 4 \frac{L_y^2}{L_x^2} + \frac{L_z'^2}{L_x^2} \geq 3. \quad (27)$$

\square

C. Power Gain over Optimal Far-Field Solution

Next, the possible power gain of employing the proposed optimal antenna positioning over the optimal far-field position is quantified. The ideal position for all transmit antennas under the far-field assumption lies in the centre of \mathcal{X} . This follows from approximating the path losses corresponding to different transmit antennas with a constant value which is analogous to the co-located transmit antenna architecture where the optimal transmit antenna positions are $a_1^* = a_2^* = 0$. The performance gain η which is obtained by designing the system using the exact SWM instead of the approximated PWM depends on the geometry of the environment. Therefore, the gain η is computed by comparing the performance of using the optimal transmit antenna locations in the Fresnel region (22) to the

optimal ones for the far-field, which are obtained by placing both antennas at zero.

Corollary 2. *The gain that is obtained by using the optimal transmit antenna placement depends on the geometry of the environment and is given by*

$$\eta = \begin{cases} \frac{12 \frac{L_y^2}{L_x^2} + 3 \frac{L_z'^2}{L_x^2} + 3}{16 \frac{L_y^2}{L_x^2} + 4 \frac{L_z'^2}{L_x^2} + 1} & \text{if } 4 \frac{L_y^2}{L_x^2} + \frac{L_z'^2}{L_x^2} \leq \frac{5}{4}, \\ \frac{\left(4 \frac{L_y^2}{L_x^2} + \frac{L_z'^2}{L_x^2} + 1\right)^{\frac{3}{2}} + 4 \frac{L_y^2}{L_x^2} + \frac{L_z'^2}{L_x^2} + 1}{16 \frac{L_y^2}{L_x^2} + 4 \frac{L_z'^2}{L_x^2}} & \text{if } \frac{5}{4} \leq 4 \frac{L_y^2}{L_x^2} + \frac{L_z'^2}{L_x^2} \leq 3, \\ 1 & \text{if } 4 \frac{L_y^2}{L_x^2} + \frac{L_z'^2}{L_x^2} \geq 3. \end{cases} \quad (28)$$

Proof. The optimal objective value is given by (25)-(27) and depends on the geometry of the environment. In the far-field, the worst receiver position lies at the boundaries of \mathcal{X} since the antennas are placed at $x = 0$. Thus, the objective value of the far-field solution corresponds to (27). \square

D. Systems with $N_t > 2$

The methodology outlined in this paper may be extended to systems with a larger number of transmit antennas, i.e., $N_t > 2$. By virtue of the max-min problem, an asymmetrical transmit antenna placement is suboptimal. Therefore, for an uneven number of transmit antennas N_t , one optimal transmit antenna position must lie in the centre of \mathcal{X} . Moreover, when N_t is even, Proposition 2 must hold for pairs of transmit antennas to ensure a symmetrical transmit antenna placement. The approach for identifying all critical receiver positions in $\mathcal{X}^{\text{crit}}$ may be cumbersome for large N_t , as the number of critical positions $|\mathcal{X}^{\text{crit}}|$ is expected to grow with N_t . Consequently, the number of transition points, which are necessary for formulating the optimal positions, is expected to grow. Alternatively, the optimal transmit antenna placement may then be obtained by solving (10) numerically. A numerical method of solving the problem is discussed at the end of Section IV-A.

IV. RESULTS AND PERFORMANCE EVALUATION

A. Optimal Position of a_1^*

The optimal position of a_1^* (22) is visualised as a function of the geometry of the system in Fig. 2. To this end, the optimal position of a_1^* is depicted as a function of one variable and one parameter. The optimal position a_1^* is given as a function of L_y/L_x , i.e., $a_1^*(L_y/L_x)$, while the value of L_z'/L_x is fixed and the parameter value is indicated by the legend entry corresponding to the respective plot. The function $a_1^*(L_y/L_x)$ is plotted by considering the parameter values $L_z'/L_x = \{0, \sqrt{5}/8, \sqrt{5}/4, 3\sqrt{5}/8, \sqrt{5}/2\}$. The parameter values are chosen to represent the boundaries of the possible geometrical ratios of the environment. For $L_z'/L_x = 0$, the environment collapses into a two-dimensional room. The maximum value $L_z'/L_x = \sqrt{5}/2$ follows from the condition in Lemma 3.

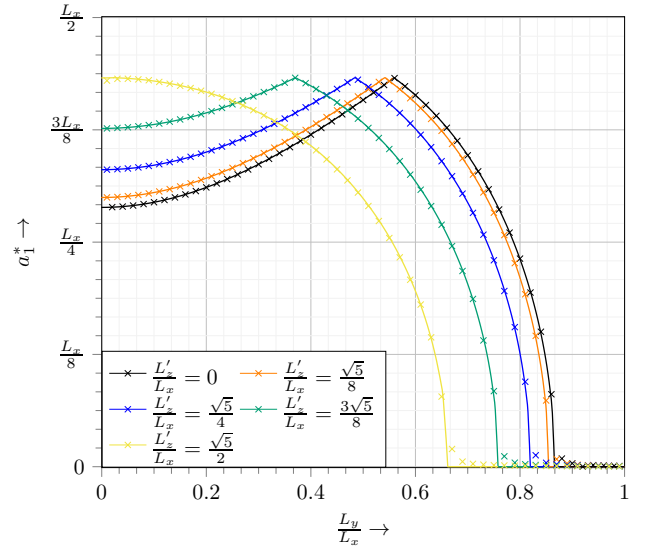


Fig. 2: Optimal placement of antenna a_1^* (22).

Fig. 2 provides insight into how the geometrical properties of the environment impact the optimal transmit antenna positions. By basing the proposed method on the SWM, an optimal solution was obtained which is capable of capturing the effects in the Fresnel region and naturally converges to the far-field solution as $4L_y^2/L_x^2 + L_z'^2/L_x^2$ grows. In the far-field, the impact of the spherical nature of the EM wavefronts at the worst receiver locations diminishes and the PWM becomes sufficiently accurate. Consequently, when the optimal solution for the Fresnel region coincides with the far-field solution, i.e., $4L_y^2/L_x^2 + L_z'^2/L_x^2 \geq 3$, then the WPT system does not have to be designed for the Fresnel region. However, for $4L_y^2/L_x^2 + L_z'^2/L_x^2 \leq 3$, designing the system for the Fresnel region has to be ensured, which requires considering the relationship between the wavelength and the distance between the transmit antennas in comparison to their distance from the receiver. The analytical solution was validated by solving the problem numerically. To this end, the quadratic form method in [20] for Fractional Programming was extended to max-min-sum-ratio problems and a sequence of parameterised convex optimisation problems was solved using CVXPY [21]. The numerical results are indicated by the crosses overlaying the respective analytical results in Fig. 2. Fig. 2 also shows that the numerical method suffers from numerical inaccuracies as the optimal a_1^* approaches 0.

B. Power Gain over Far-Field Solution

The power gain η in (28) is visualised in Fig. 3 as a function of L_y/L_x , while fixing the parameter L_z'/L_x for every plot of the function. The values of the parameters are identical to the ones listed in Subsection IV-A. The maximum gain is three and is achieved for $L_y/L_x \rightarrow 0$ with $L_z'/L_x = 0$. Consequently, using the proposed optimal positioning based on the SWM provides up to three times the amount of received power compared to the far-field approach. As the impact of

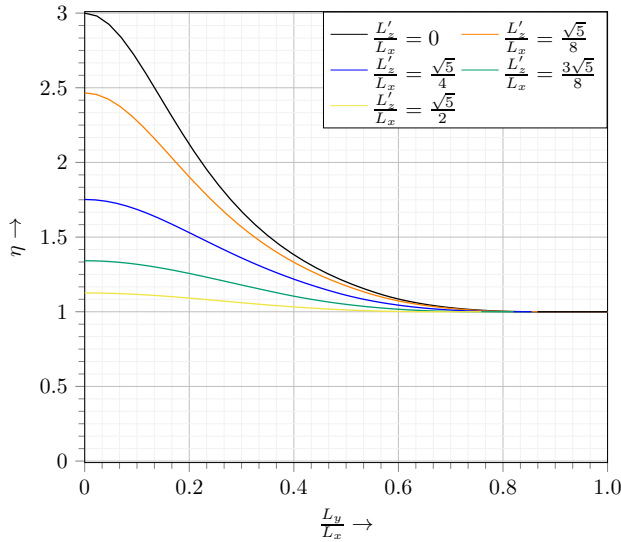


Fig. 3: Possible power gain η (28).

the spherical nature of the EM wavefronts decreases, the gain over the far-field solution drops.

V. CONCLUSION

In this paper, we considered a MISO WPT system that comprises a two-antenna energy transmitter and a single antenna energy receiver under LoS conditions. Hereby, the objective was the maximisation of the received power for the worst possible receiver position by identifying the optimal transmit antenna deployment. The approach in this paper leverages the symmetry among the positions of the transmit antennas. The symmetry is a necessary constraint in order to avoid biasing certain receiver positions over others, as this would lead to a worse objective globally. The proposed optimal, analytical solution provides insight into how the geometry impacts the optimal placement of the transmit antennas. Our solution reveals that distributing the transmit antennas in the environment is optimal when in any location of the environment the PWM is not a suitable approximation of the SWM. Otherwise, a co-located antenna architecture is optimal which corresponds to the optimal solution for the far-field. The solution was validated by solving the problem numerically. Furthermore, the maximum power gain over the far-field solution was found to be three. The extensions of the proposed solution to small-scale fading channels, multiple transmit antennas, and more flexible transmit antenna placements are interesting topics for future work.

REFERENCES

- [1] H. Zhang, N. Shlezinger, F. Guidi, D. Dardari, and Y. C. Eldar, "6G Wireless Communications: From Far-field Beam Steering to Near-field Beam Focusing," 2022.
- [2] H. Zhang, N. Shlezinger, F. Guidi, D. Dardari, M. F. Imani, and Y. C. Eldar, "Beam Focusing for Near-Field Multiuser MIMO Communications," *IEEE Trans. Wireless Commun.*, vol. 21, pp. 7476–7490, Sept. 2022.

- [3] H. Zhang, N. Shlezinger, F. Guidi, D. Dardari, M. F. Imani, and Y. C. Eldar, "Near-Field Wireless Power Transfer for 6G Internet of Everything Mobile Networks: Opportunities and Challenges," *IEEE Commun. Mag.*, vol. 60, pp. 12–18, Mar. 2022.
- [4] H. Zhang, N. Shlezinger, F. Guidi, D. Dardari, M. F. Imani, and Y. C. Eldar, "Near-Field Wireless Power Transfer with Dynamic Metasurface Antennas," in *2022 IEEE 23rd Int. Workshop Signal Process. Advances Wireless Commun.*, pp. 1–5, 2022.
- [5] A. Massa, G. Oliveri, F. Viani, and P. Rocca, "Array Designs for Long-Distance Wireless Power Transmission: State-of-the-Art and Innovative Solutions," *Proc. IEEE*, vol. 101, pp. 1464–1481, June 2013.
- [6] C. R. Valenta and G. D. Durgin, "Harvesting Wireless Power: Survey of Energy-Harvester Conversion Efficiency in Far-Field, Wireless Power Transfer Systems," *IEEE Microw. Mag.*, vol. 15, pp. 108–120, June 2014.
- [7] A. Costanzo and D. Masotti, "Smart Solutions in Smart Spaces: Getting the Most from Far-Field Wireless Power Transfer," *IEEE Microw. Mag.*, vol. 17, pp. 30–45, May 2016.
- [8] B. Clerckx, K. Huang, L. R. Varshney, S. Ulukus, and M.-S. Alouini, "Wireless Power Transfer for Future Networks: Signal Processing, Machine Learning, Computing, and Sensing," *IEEE J. Sel. Topics Signal Process.*, vol. 15, pp. 1060–1094, Aug. 2021.
- [9] B. Clerckx, R. Zhang, R. Schober, D. W. K. Ng, D. I. Kim, and H. V. Poor, "Fundamentals of Wireless Information and Power Transfer: From RF Energy Harvester Models to Signal and System Designs," *IEEE J. Sel. Areas Commun.*, vol. 37, pp. 4–33, Jan. 2019.
- [10] B. Clerckx, J. Kim, K. W. Choi, and D. I. Kim, "Foundations of Wireless Information and Power Transfer: Theory, Prototypes, and Experiments," *Proc. IEEE*, vol. 110, pp. 8–30, Jan. 2022.
- [11] X. Gu, S. Hemour, and K. Wu, "Far-Field Wireless Power Harvesting: Nonlinear Modeling, Rectenna Design, and Emerging Applications," *Proc. IEEE*, vol. 110, pp. 56–73, Jan. 2022.
- [12] L. Liu, R. Zhang, and K.-C. Chua, "Multi-Antenna Wireless Powered Communication With Energy Beamforming," *IEEE Trans. Commun.*, vol. 62, pp. 4349–4361, Dec. 2014.
- [13] K. W. Choi, A. A. Aziz, D. Setiawan, N. M. Tran, L. Ginting, and D. I. Kim, "Distributed Wireless Power Transfer System for Internet of Things Devices," *IEEE Internet Things J.*, vol. 5, pp. 2657–2671, Aug. 2018.
- [14] S. Shen, J. Kim, C. Song, and B. Clerckx, "Wireless Power Transfer With Distributed Antennas: System Design, Prototype, and Experiments," *IEEE Trans. Ind. Electron.*, vol. 68, pp. 10868–10878, Nov. 2021.
- [15] H. Do, S. Cho, J. Park, H.-J. Song, N. Lee, and A. Lozano, "Terahertz Line-of-Sight MIMO Communication: Theory and Practical Challenges," *IEEE Commun. Mag.*, vol. 59, pp. 104–109, Mar. 2021.
- [16] X. Li, H. Lu, Y. Zeng, S. Jin, and R. Zhang, "Near-Field Modeling and Performance Analysis of Modular Extremely Large-Scale Array Communications," *IEEE Commun. Lett.*, vol. 26, pp. 1529–1533, July 2022.
- [17] D. Tse and P. Viswanath, *Fundamentals of Wireless Communication*. Cambridge, UK: Cambridge University Press, 2005.
- [18] R. Zhang and C. K. Ho, "MIMO Broadcasting for Simultaneous Wireless Information and Power Transfer," *IEEE Trans. Wirel. Commun.*, vol. 12, pp. 1989–2001, May 2013.
- [19] I. N. Bronstein, K. A. Semendjajew, G. Musiol, and H. Mühlig, *Taschenbuch der Mathematik*. Haan-Gruiten, DE: Verlag Europa-Lehrmittel, 2016.
- [20] K. Shen and W. Yu, "Fractional Programming for Communication Systems - Part I: Power Control and Beamforming," *IEEE Trans. Signal Process.*, vol. 66, pp. 2616–2630, May 2018.
- [21] S. Diamond and S. Boyd, "CVXPY: A Python-Embedded Modeling Language for Convex Optimization," *J. Mach. Learn. Res.*, vol. 17, pp. 1–5, Mar. 2016.